Journal of Nuclear and Particle Physics 2014, 4(1): 25-30
DOI: 10.5923/j.jnpp.20140401.04

Nuclei at or Near Drip-Lines

Harvinder Kaur[1], M. S. Mehta[2,*]

[1]Department of Appleid Sciences, RBCEBTW, Mohali-140 104, India
[2]King's Group of Institutions, Barnala-148 101, India

Abstract The magic number and halo and /or skin (neutron) of the nuclei at or near neutron drip-line are studied using axially deformed relativistic mean field model with NL3 and NL3* parameter sets. The density profiles of some of selected nuclei in the light mass region of nuclear landscape are plotted for the purpose. A considerable difference in the densities of neutron and proton can be seen easily in all the cases studied. Also, single particle energy levels show the visible shell gaps at N = 28 and 40 which corresponds the sudden decrease in the two neutron separation energy. The two results are consistent with each other, while the shell gaps corresponding to the numbers N = 32 and 34 seem not to be supporting the magicity at these numbers in the isotopes considered here.

Keywords Relativistic Mean Field, Shell Structure, Magic Number, Halo, Skin, Drip-line, Quadrupole Deformation

1. Introduction

The study of neutron-rich nuclei with unusually large N/Z ratios is challenging the conventional view of nuclear structure. In the recent decades nuclear structure physics has made a considerable progress by the discovery of new phenomena and the emergence of new frontiers. The availability of more energetic beams of short-lived (radioactive) nuclei of the rare isotopes or exotic nuclear beams, has opened up the way for the exploration of the structure and dynamics of nuclei in drip-line regions, where very limited information is available. The advancement in the radioactive ion beam facilities enables us to study the behavior of nuclei near or even beyond the neutron and proton drip-lines and to investigate the emergence of new modes of nuclear behavior.

The most fascinating phenomena found in exotic nuclei are the nuclear halo, skin and the new sequence of magic numbers than the nuclei on the beta-stability line of the nuclear landscape. The other interesting features in nuclei close to neutron drip-line are for example largely extended spatial density distribution, coupling of the bound states to the continuum, the Borromean structure etc. The experimental observation of large nuclear matter distribution of ^{11}Li[1] nucleus started the chapter of the exotic properties of the nuclei in the region away from beta-stability line. This new phenomenon was termed as the halo. The definition of a halo nucleus is still being debated, but at least three basic conditions must be fulfilled[2]: (i) low separation energy of the valance particle (or particle clusters); (ii) a wave function be in a low relative angular momentum state (preferably s-wave); (iii) decoupling from the core. The halo structure in nuclei can develop when the system approaches the threshold and the relative motion is not constrained by a strong long-range repulsive force. As a result the tail of the wave function extends out well beyond the region of nuclear interaction, generating an unusual outer region of low nuclear density. The physics of neutron-rich nuclei is one of the current topics in nuclear science. In the past, several theoretical model in relativistic kinematics such as Hartree Bogoliubov with or without the Fock term, Relativistic mean field model with hartree approximation have been developed for a self-consistent description of spherical as well as deformed halo nuclei[3,4].

The reaction cross sections of certain nuclei ^{6,8}He, ^{11}Li[1] and ^{11,14}Be[5] have been found anomalously large. The matter radius of such nuclei is much larger than that of neighboring nuclei. These are the two neutron halo nuclei. Recently, the measurement of nuclear reaction cross-section for ^{19,20,22}C[6] shows that the drip-line nucleus ^{22}C has halo structure. Also, the isotopes of ^{42,44}Mg nuclei close to neutron drip-line also have been predicted[7, 8] to be halo. The nucleus ^{11}Be, ^{19}C, ^{31}Ne are the examples of one-neutron halo nucleus[9, 10]. The density distribution showing an extended tail with a diffused neutron skin and neutron halo can be seen in references[11, 12].

The change in magic number is another interesting feature of the nuclei in the drip-line region. It is now established that the dynamic effects of nucleon-nucleon interaction result in the evolution of shell structure and hence the new magic number sequence in drip-line region. The motivation for the present work is the investigation of dynamism of the magic numbers in neutron drip-line to the conventional ones at stability line. The halo structure of nuclei is another property of the nuclei at neutron drip-line. The extent of halo

* Corresponding author:
mehta_iop@yahoo.co.uk (M. S. Mehta)
Published online at http://journal.sapub.org/jnpp

character in the isotopes is varying for different calculations.

2. Formalism

We use axially deformed relativistic mean field (RMF) model to study the properties of the nuclei. The RMF model has been proved to be a very powerful tool to explain the properties of finite nuclei and infinite nuclear matter[13, 14, 15] for the last two decades. We start with the relativistic Lagrangian density for a nucleon-meson many-body system,

$$\begin{aligned}\mathcal{L} &= \overline{\psi_i}\{i\gamma^\mu\partial_\mu - M\}\psi_i + \frac{1}{2}\partial^\mu\sigma\partial_\mu\sigma - \frac{1}{2}m_\sigma^2\sigma^2 \\ &- \frac{1}{3}g_2\sigma^3 - \frac{1}{4}g_3\sigma^4 - g_s\overline{\psi_i}\psi_i\sigma - \frac{1}{4}\Omega^{\mu\nu}\Omega_{\mu\nu} \\ &+ \frac{1}{2}m_w^2V^\mu V_\mu + \frac{1}{4}c_3(V_\mu V^\mu)^2 - g_w\overline{\psi}_i\gamma^\mu\psi_iV_\mu \\ &- \frac{1}{4}\vec{B}^{\mu\nu}.\vec{B}_{\mu\nu} + \frac{1}{2}m_\rho^2\vec{R}^\mu.\vec{R}_\mu - g_\rho\overline{\psi}_i\gamma^\mu\vec{\tau}\psi_i.\vec{R}^\mu \\ &- \frac{1}{4}F^{\mu\nu}F_{\mu\nu} - e\overline{\psi}_i\gamma^\mu\frac{(1-\tau_{3i})}{2}\psi_iA_\mu.\end{aligned} \quad (1)$$

The field for the σ-meson is denoted by σ, that for the ω-meson by Vμ and for isovector ρ-meson by Rμ. A^μ denotes the electromagnetic field. The ψ_i are Dirac spinors for nucleons whose third component of isospin is denoted by τ_{3i}. Here g_s, g_w, g_ρ and $e^2/4\pi$ =1/137 are the coupling constants for σ, ω, ρ mesons and photon, respectively. g_2, g_3 and c_3 are the parameters for the nonlinear terms of σ- and ω-mesons. M is the mass of the nucleon and m_σ, m_ω and m_ρ are the masses of the σ, ω and ρ-mesons, respectively. $\Omega_{\mu\nu}$, $B^{\mu\nu}$ and $F^{\mu\nu}$ are the field tensors for V^μ, R^μ and photon fields, respectively[4].

From the relativistic Lagrangian we get the field equations for the nucleons and mesons. These equations are solved by expanding the upper and lower components of Dirac spinors and the Boson fields in a deformed harmonic oscillator basis with an initial deformation. The set of coupled equations is solved numerically by a self-consistent iteration method. The centre-of-mass motion is estimated by the usual harmonic oscillator formula $E_{c.m.}=3/4(41A^{-1/3})$. The quadrupole deformation parameter β_2 is evaluated from the resulting quadrupole moment[4] using the formula,

$$Q = Q_n + Q_p = \sqrt{\frac{9}{5\pi}}AR^2\beta_2 \quad (2)$$

Where, $R=1.2A^{1/3}$. The total binding energy of the system is,

$$\begin{aligned}E_{total} &= E_{part} + E_\sigma + E_\omega + E_\rho \\ &+ E_c + E_{pair} + E_{c.m.}\end{aligned} \quad (3)$$

where E_{part} is the sum of the single-particle energies of the nucleons and E_σ, E_ω, E_ρ, E_c and E_{pair} are the contributions of the mesons fields, the Coulomb field and the pairing energy, respectively. For the open shell nuclei, effect of pairing interactions is added in the BCS formalism. The pairing gaps for proton (Δ_p) and neutron (Δ_n) are calculated from the relations[16],

$$\begin{aligned}\triangle_p &= rb_sZ^{-1/3}e^{\left(sI-tI^2\right)} \\ \triangle_n &= rb_sN^{-1/3}e^{-\left(sI+tI^2\right)}\end{aligned} \quad (4)$$

where r=5.72 MeV, s=0.118, t=8.12, b_s=1 and I=(N-Z)/(N+Z).

3. Results and Discussion

In the present calculations we make use of axially deformed relativistic mean field (RMF) model with NL3 (non-linear coupling) and NL3* parameter sets. There are a number of parameter sets used in RMF, out of which NL3[17] and newer set NL3*[18] are found to be producing better results for the calculations of the ground state properties of nuclei. The detail of the parameter sets is shown in Table 1. The parameters are obtained by fitting the nuclear matter properties for closed sell nuclei such as ^{16}O, ^{40}Ca, ^{48}Ca and ^{208}Pb etc.

Table 1. NL3 and NL3* parameter sets

Parameter	NL3	NL3*
M (MeV)	939.0	939.0
m_σ (MeV)	508.1941	502.5742
m_ω (MeV)	782.501	782.6
m_ρ (MeV)	763.0	763.0
g_σ	10.2169	10.0944
g_ω	12.8675	12.8065
g_ρ	4.4744	4.5748
g_2 (fm^{-1})	-10.4307	-10.8093
g_3	-28.8851	-30.1486

We have taken few representative cases (Ca, Si, Mg and C) in the light mass region near the neutron drip-line of nuclear landscape to study the halo and /or skin and the magic numbers. The outcome of the calculations is discussed as under:

The density profile, two-neutron separation energy and single particle energy are plotted in the figures.

The Fig. 1 shows the neutron and proton density distribution of $^{50\text{-}56}$Ca nuclei with neutron numbers N = 30, 32, 34, 36. There is a considerable difference between the neutron density and the proton density at the tail part of these isotopes. The difference increases with the increase in the neutron number. The extended tail in the neutron density gives the indication of halo or neutron skin. This exotic phenomenon was first measured experimentally in 1985 by I. Tanihata et al.[1] in ^{11}Li a nucleus of very light mass region and was termed as halo for the first time. Now, other nuclei having halo and/or skin of the neutrons are found. The

different models show slight difference in the magnitudes of neutron and proton densities at the tail part of the density profile.

Another phenomenon of particular interest is the magicity at proton/ neutron number N = Z = 28 and N = 32 and 40 near the neutron drip-line in Ca and Ni-isotopes, which has been a center of discussion for sometimes now (see Ref.[19], and the references therein). The measurements showed some surprising changes in the nuclear shell structure as a function of proton and neutron numbers in light nuclei. These observations triggered numerous theoretical investigations, which in turn made new predictions that some magic numbers disappear and new shell gaps appear in certain regions of the nuclear chart[20] away from the beta-stability line.

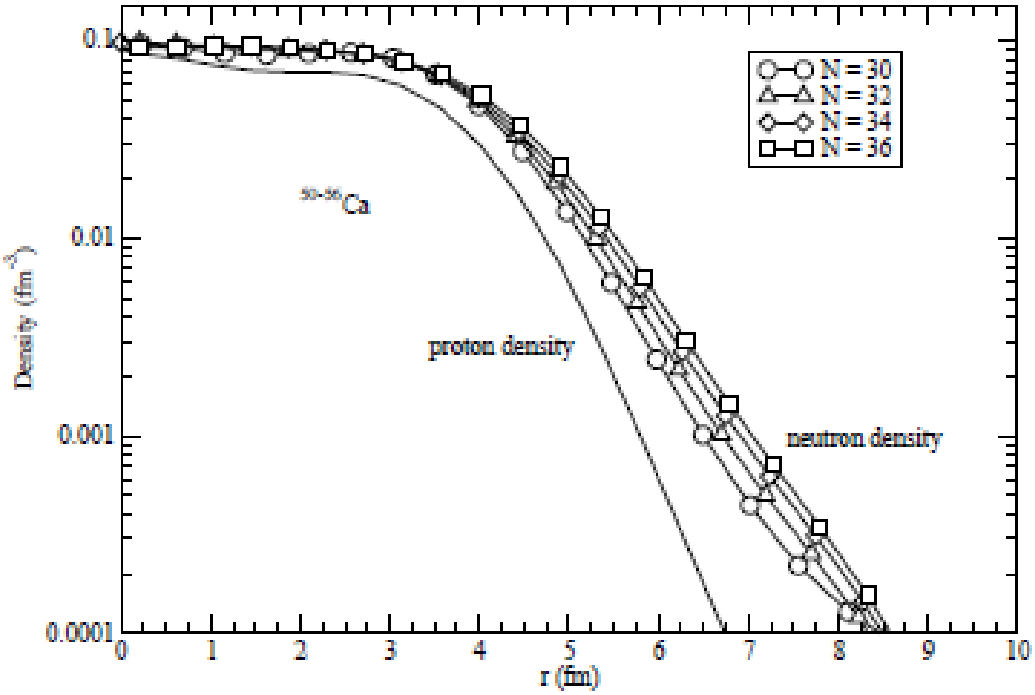

Figure 1. The density distribution of $^{50-56}$Ca nuclei with NL3 parameter set

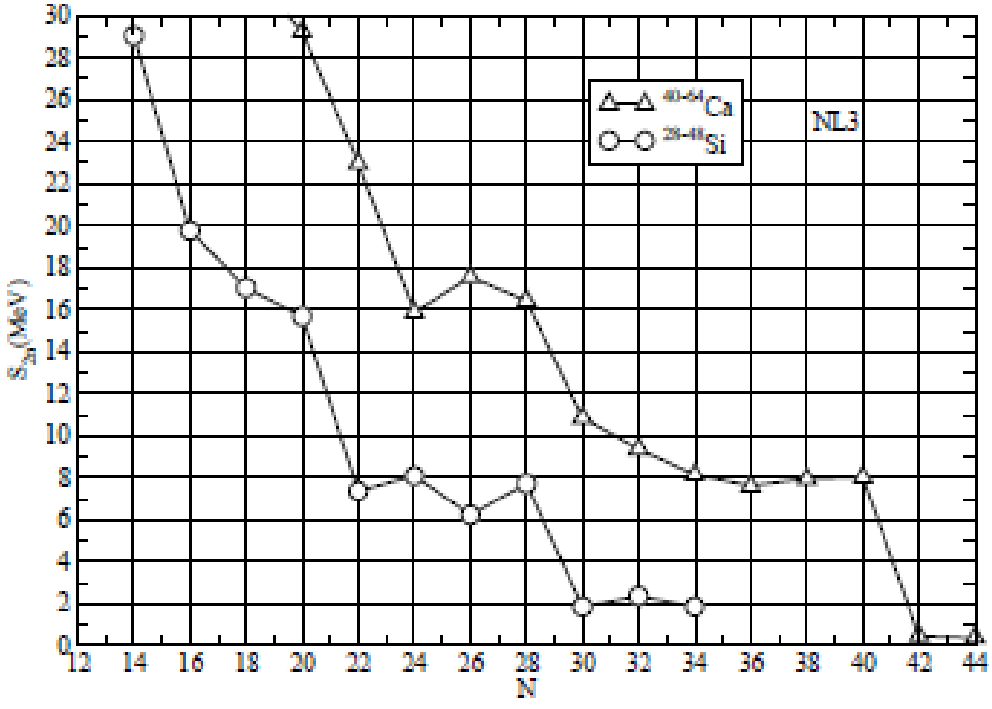

Figure 2. The two neutron separation energy for Si and Ca-isotopes using NL3 parameter set

The first evidence for N = 16 to be magic number in oxygen was observed from an evaluation of neutron separation energies on the basis of measured masses[21]. The new magic number at N = 32 has been observed experimentally by Kanungo et al. ^{54}Ca[22] recently. But theoretically, shell model with new effective interaction GXPF1 (G-matrix effective interaction for pf-shell nuclei) and monopole component of tensor interaction, predict the shell closure at N = 34[23]. However, the well-established interactions KB3G[24] (an effective interaction, the detail can be found in ref.[25]) and the spherical Hartree-Fock calculations with the semi-realistic NN interactions[26] give the shell closer at N = 32. Therefore, it is interesting to investigate the shell closer at N = 32 and 34 for ^{54}Ca isotope using RMF model. The shell gaps at these particular numbers are not pronounced in the present calculations as is clear from the Fig. 2 and Fig. 3. The two neutron separation energy for Si and Ca-isotopes are plotted in Fig. 2. The sudden fall in the two-neutron separation energy at any number shows extra stability at that particular number. From the figure it is clear that the sharp decrease in separation energy is at N = 14, 20 and 28 in case of Si and at N = 20, 28 and 40 in case of Ca.

The change in magic numbers in nuclei of light mass region close to drip-lines is experimentally observed[21, 22]. In order to visualize the shell arrangement of the nucleons, single particle energy levels for $^{52, 60}$Ca isotopes are plotted in Fig. 3. The shell gaps at these numbers correspond to the sharp fall in separation energy as shown in Fig. 2.

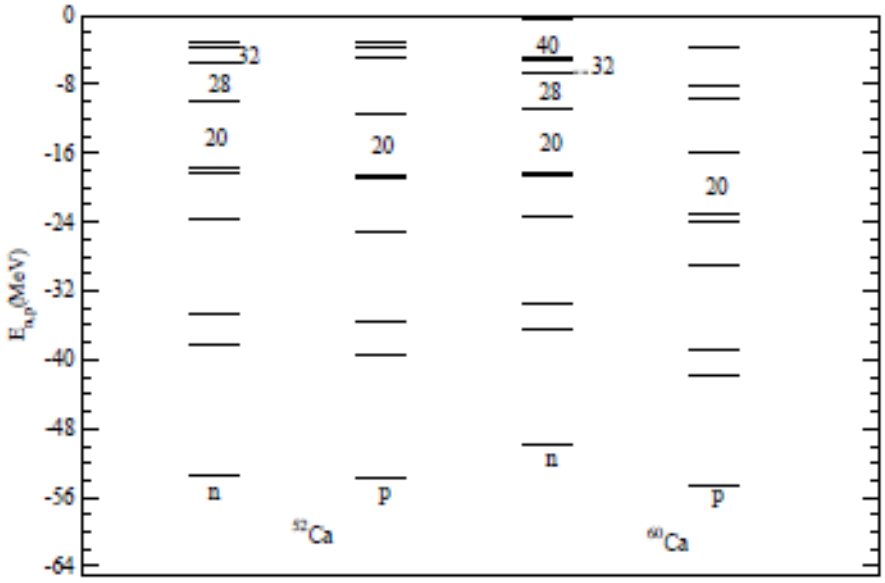

Figure 3. The single particle energy levels of neutrons and protons for ^{52,60}Ca nuclei using NL3 parameter

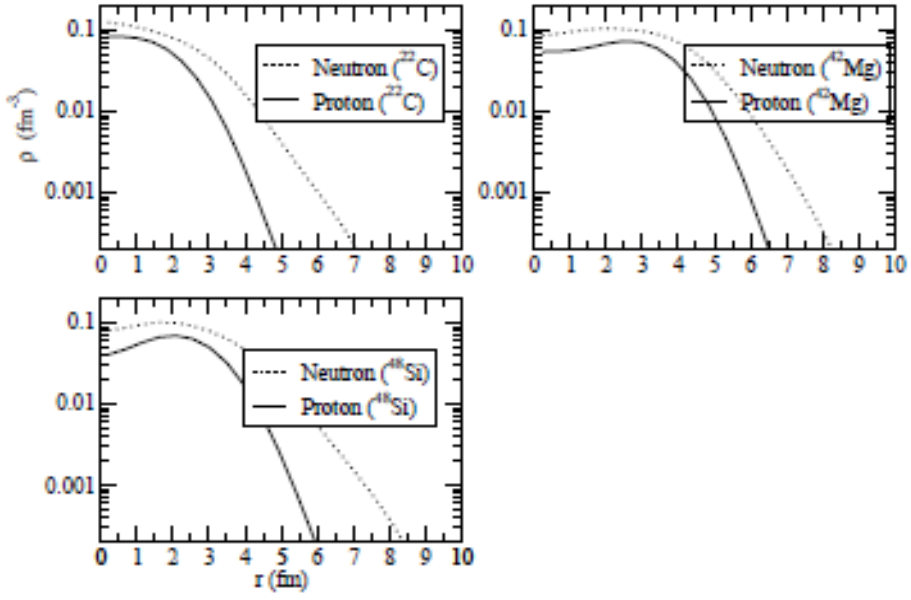

Figure 4. The density distribution of ^{22}C, ^{42}Mg and ^{48}Si nuclei with NL3 parameter set

The density distribution of ^{48}Si nucleus is shown in Fig. 4, which clearly shows the considerable difference in the neutron and proton densities. Recently, the observation of new halo ^{22}C nucleus has further added another dimension to the nuclear structure. This case is of special interest because an isotope ^{21}C inside the drip-line is unstable. Also, ^{19}C is one neutron halo and can be treated as two body halo. The nuclei such as ^{6}He and ^{11}Li are three-body halos and their properties make them Borromean type nuclei. In case of ^{22}C, there are 16 neutrons i.e. N = 16, which is new magic number in neutron-rich systems. The density profile of ^{22}C, ^{42}Mg and ^{48}Si nuclei shown in Fig. 4, clearly indicate the halo structure owing to the considerable difference in the neutron and proton densities at the tail.

4. Conclusions

In conclusion, we investigate the quite dramatic changes in the shell structure on nuclei in the neutron drip-line region using axially deformed relativistic mean field model with NL3 and NL3* parameter sets. Here, we investigate the halo character and the magic number in the nuclei close to or on the neutron drip-line. The density profiles show that the nuclei considered here are having considerable difference in the densities of neutron and proton, which is a clear indication of halo structure. The other part of investigation is magic number in this mass region. The figure 3, shows the single particle energy levels of ^{52}Ca and ^{60}Ca for both neutron and proton. There are visible shell gaps at N = 28 and 40 which correspond to the sudden decrease in two neutron separation energy in figure 2. The two results are consistent with each other. The shell gap corresponding to the numbers N = 32 and 34 seem not to be supporting the magicity in these isotopes. The shells at N = 32 or 34 are separated by energy ~1.6 MeV only, as compared to the gaps of ~4.5 MeV at N = 28. The shell gap of ~1.6 is small enough to create the stability required for the number to be a magic number. Therefore, these numbers do not seem show the magic number character.

ACKNOWLEDGEMENTS

One of the authors HK thanks Rayat Bahra Group of Institutes for partial financial support of the present work. MSM thanks Dr. S. K. Patra for the discussion and valuable suggestions.

REFERENCES

[1] I. Tanihata et al., Measurements of Interaction Cross Sections and Nuclear Radii in the Light p-Shell Region, Phys. Rev. Lett. 55, 2676 (1985).

[2] J. S. Al-Khalili, An Introduction to Halo Nuclei, Lect. Notes Phys. 651,77 (2004).

[3] J. Meng and P. Ring, Relativistic Hartree-Bogoliubov Description of the Neutron Halo in ^{11}Li, Phys. Rev. Lett. 77, 3963 (1996); W. H. Long et al., Relativistic Hartree-Fock-Bogoliubov theory with density dependent meson-nucleon couplings, Phys. Rev. C 81, 024308 (2010).

[4] Y. K. Gambhir, P. Ring and A. Thimet, Relativistic Mean Field Theory for Finite Nuclei, Ann. Phys. 198, 132 (1990).

[5] Tanihata I. et al., Determination of the density distribution and the correlation of halo neutrons in ^{11}Li, Phys. Lett., B 287, 307 (1992).

[6] K. Tanaka et al., Observation of a Large Reaction Cross Section in the Drip-Line Nucleus ^{22}C, Phys. Rev. Lett., 104, 062701 (2010).

[7] L. Li et al., Halos in a deformed Relativistic Hartree-Bogoliubov Theory in Continuum, Phys. Rev. C 85, 024312 (2012).

[8] Zhou et al., Odd systems in deformed relativistic Hartree Bogoliubov Thery in Continuum, Phys. Rev. C 82, 011301R (2010).

[9] T. Nakamura et al., Experimental Program on Halo Nuclei with non-accelerated beams, Phys. Rev. Lett. 103, 262501 (2009).

[10] A. Di Pietro, et. al., Elastic Scattering and Reaction Mechanisms of the Halo Nucleus 11Be around the Coulomb Barrier, Phys. Rev. Lett. 105, 022701 (2010).

[11] I. Tanihata, J. Phys. G, Neutron halo nuclei, 22, 157 (1996); I. Tanihata et al., Measurements of Interaction Cross Sections and Nuclear Radii in the Light p-Shell Region, Phys. Rev. Lett. 55, 2676 (1985).

[12] K. Riisager, Nuclear halo states, Rev. Mod. Phys. 66, 1105 (1994); Tanihata I. et al., Revelation of thick neutron skins in nuclei, Phys. Lett. B 289, 261 (1992); Tanihata I., Prog. Part. Nucl. Phys. 35, 505 (1995).

[13] R. Machleidt, The meson theory of nuclear forces and nuclear structure, Adv. Nucl. Phys. 19, 189 (1989).

[14] S. K. Patra and C. R. Praharaj One neutron removal reaction using relativistic mean field densities, Phys. Rev. C 44, 2552 (1991).

[15] M. Del Estal, M. Centelles, X. Vi\~nas and Patra S. K., Versatility of field theory motivated nuclear effective Lagrangian approach, Phys. Rev. C 63, 024314 (2001).

[16] D. G. Madland and J. R. Nix, New model of the average neutron and proton pairing gaps, Nucl. Phys. A 476, 1 (1988).

[17] G. A. Lalazissis, J. Konig and P. Ring, Phys. Rev. C 55, 540 (1997).

[18] G. A. Lalazissis, S. Karatzikos, R. Fossion, D. Pena Arteaga, A. V. Afanasjev, and P. Ring, Phys. Lett. B 671, 36 (2009).

[19] Sorlin O. and Porquet M. -G., Nuclear magic numbers: new features far from stability, Prog. Part. Nucl. Phys. 61, 602 (2008); Sorlin O., et al., $^{68}_{28}40_{40}$: Magicity versus Super fluidity, Phys. Rev. Lett. 88, 092501 (2002).

[20] R. Krücken, New magic numbers, arXiv:1006.2520 v1[phys.pop-ph], 2010.

[21] A. Ozawa, et al., New Magic Number, N = 16, near the

Neutron Drip Line, Phys. Rev. Lett. 84 5493 (2000); R. Kanungo, I. Tanihata and A. Ozawa, Observation of new neutron and proton magic numbers, Phys. Lett. B 528, 58 (2002).

[22] R. Kanungo, I. Tanihata and A. Ozawa, Observation of new neutron and proton magic numbers, Phys. Lett. B 528 58 (2002); J. I. Prisciandaro et al., Observation of new neutron and proton magic numbers, Phys. Lett. B 510, 17 (2001).

[23] M. Honma, T. Otsuka, B. A. Brown, Mizusaki T., Effective interaction for pf-shell nuclei, Phys. Rev. C 65, 061301(R) (2002).

[24] E. K. Warburton, J. A. Becker, and B. A. Brown, Mass systematics for A=29–44 nuclei: The deformed A∼32 region, Phys. Rev. C 41}, 1147 (1990); A. Poves et al., Nucl. Phys. A 694, 157 (2001).

[25] T. T. S. Kuo, G. E. Brown, Nucl. Phys. A 114, 241 (1968).

[26] H. Nakada, One neutron removal reaction using relativistic mean field densities, arXiv:1003.572v2[nucl-ph], 2010.